Direct Conversion CdZnTe and CdTe Detectors for Digital Mammography

Shi Yin, Tümay O. Tümer, Dale Maeding, James Mainprize, Gord Mawdsley, Martin J. Yaffe, Eli E. Gordon, and William J. Hamilton

***Abstract*—Hybrid CdZnTe and CdTe pixel detector arrays with 50 × 50 micron^2 pixel sizes that convert x-rays directly into charge signals are under development at NOVA for applications to digital mammography. CdZnTe and CdTe have superior x-ray quantum efficiency compared to either emulsion-based film, phosphor-based detectors or other low-Z, solid-state detectors such as silicon. In this paper, latest results from thin (0.15 to 0.2 mm) CdZnTe and CdTe detectors will be presented in terms of modulation transfer function (MTF), detective quantum efficiency (DQE), and phantom images. Single-crystal CdZnTe detectors yield better results in DQE as well as phantom images, compared to the polycrystalline CdZnTe detectors. This is due to the nonuniformities in the polycrystal that degrade the charge transport properties. Because of the charge-coupling limitation of the readout ASIC that was originally designed for Si detectors, the detector is biased to collect holes from the front side. This charge collection mode limits the CdZnTe detector performance. Their DQE measurements yield 25% and 65% for the poly-crystal and single-crystal CdZnTe detectors respectively. Poly-crystal CdTe test detectors were also hybridized to the same type charge readout chip. Since CdTe has much longer hole-propagation lengths compared to CdZnTe, it shows better performance in the hole-collecting mode. However, severe polarization effect degrades performance of the present device. Excellent images were also obtained from the CdTe detectors. Future work to redesign the readout ASIC and, thus, improve the detector performance is discussed. Application to industrial imaging such as nondestructive evaluation (NDE) and nondestructive inspection (NDI) is a natural extension.**

***Index Terms*—Digital mammography, direct convesion detectors, pixel detectors, solid-state detectors, X-ray detectors, X-ray imaging.**

I. Introduction

DIGITAL mammography offers the potential for improved image quality and the possibility of increased performance of detecting breast cancer, particularly in women with dense breasts where current screen-film mammography is often lacking. Digital mammography will also facilitate the implementation of file archiving and retrieving, computer-aided diagnosis (CAD) and telemammography [1]. Conventional x-ray film mammograms are still an effective way for screening of breast cancer, but its response to x-rays is nonlinear and the efficiency is low. Currently there are phosphor or scintillator based CCD or TFT digital mammography systems under clinical trials, but they are also less efficient compared to the direct conversion detectors due to the intermediate x-ray to light conversion process [2].

In our earlier work, 1.5-mm silicon and 2-mm-thick CdZnTe detectors were fabricated and tested using a charge-coupled device (CCD) and indium bump bonding technology [3]. Preliminary images were obtained which showed reasonably good spatial resolution and efficiency. Even though Si detectors have the advantage of easy fabrication with low cost, its low atomic number $(Z = 14)$ has the disadvantage of low x-ray absorption and thus thick materials are needed for better efficiency. Because thick Si detectors cause angle blurring as well as fabrication complications, we then turned our attention to higher atomic number detector materials, such as CdZnTe $(Z = 48, 30, 52)$ or CdTe $(Z = 48, 52)$ for our direct conversion digital mammography work.

An x-ray imaging system performance can be characterized quantitatively using two measurable parameters: modulation transfer function (MTF) and detective quantum efficiency (DQE). The MTF measures the imaging system's spatial resolution, and the DQE measures the system's efficiency in transferring the signal-to-noise ratio (SNR) (squared) contained in the incident x-ray pattern to the detector output [4]

In this work, CdZnTe and CdTe solid-state detectors are used to convert the incident x-ray photons into electron–hole (e–h) pairs. The created e–h pairs drift in opposite directions toward the electrodes, and charges are generated on the pixel pads at the front end of the detector. The charges are then read out by an application specific integrated circuit (ASIC) CCD chip. A special slot-scan time delayed integration (TDI) technique is used in the readout chip. This technology has the advantage of both charge integration and large well capacity, which meets the high dynamic range and high spatial resolution requirements for digital mammography. Charge transport properties, as well as spectral analysis, of a 0.5-mm-thick CdZnTe detector is presented. MTF and DQE measurements of several 0.15 mm to 0.2-mm-thick CdZnTe and CdTe detectors are also analyzed. Sample images from 0.15 mm to 0.2-mm-thick CdZnTe and CdTe detectors are presented, and the image quality is discussed. The adaptability of these detectors to digital mammography, as well as to nondestructive evaluation (NDE) and nondestructive inspection (NDI), is also discussed.

Manuscript received January 31, 2001; revised August 7, 2001. This work was supported by DOD Army Grant DAMD17-97-1-7255.

S. Yin and T. O. Tümer are with NOVA R&D Inc., Riverside, CA 92507 USA (e-mail: shi.yin@novarad.com).

D. Maeding is with Innovative Design, Dana Point, CA 92629 USA.

J. Mainprize, G. Mawdsley, and M. J. Yaffe are with the University of Toronto Sunnybrook and Women's Health Sciences Centre, Toronto, ON M4N 3M5, Canada.

E. E. Gordon and W. J. Hamilton are with Raytheon Systems Company, Goleta, CA 93117 USA.

Publisher Item Identifier S 0018-9499(02)01646-5.

II. METHOD

The CdZnTe and CdTe detectors are fabricated in the following steps. First, 2-mm-thick CdZnTe or CdTe detectors are indium bump bonded to the readout chip. Then the detectors are trimmed down, using a proprietary diamond point turning (DPT) technique, to a very small thickness without degrading the detector's spectroscopic properties. We have compared the ^{241}Am spectrum of a commercial pad detector to that of a DPT processed detector, and found no difference in their spectra where both detectors yield a 7% energy resolution of the 60 keV photo peak. The DPT technique thus allows us to fabricate CdZnTe and CdTe detectors down to tens of microns in thickness if necessary.

Because of the short propagation lengths for holes in CdZnTe, it is preferable to configure the detector such that the electrons travel the longest distance for good total charge collection. To test the hole-collecting inefficiency of our CdZnTe, we set up a spectroscopy test station such that the detector bias and polarity of the amplifier can be reversed to collect either holes or electrons from the same detector configuration.

Fig. 1 shows the experimental setup of the spectroscopy test station. It consists of an eV 5093 preamplifier, an ORTEC 672 shaper, and a BERTAN 230 high voltage power supply. A 0.5 mm poly-crystalline CdZnTe detector, indium bump bonded to a quartz test substrate, was used in the experiment. The experimental procedure is as follows: First, the detector system is set up either as shown in Fig. 1(a) or (b). Then the radioactive source ^{241}Am is placed as shown, where its position is fixed. The charge signals from the induced electron–hole pairs inside the detector are then amplified, shaped, and sent to a multi-channel analyzer. The spectrum is recorded in the computer. Then, without changing the position of the ^{241}Am source, the HV is reversed and so is the polarity of the shaping amplifier. A new spectrum is then recorded for the new configuration. When the HV is positive, electrons are collected in the preamplifier. When the HV is negative, holes are collected in the preamplifier. Since the channel number in the spectral analyzer is proportional to the total charge collected from each incident photon, the product of the channel number to the count number is the total charge created in that particular channel. If we sum up this product for each channel, we then obtain a result that is proportional to the total charge created in the detector. We also note that the system noise contributes to the result, but its contribution is within the accuracy of our measurements ($\sim$5%).

An ASIC chip (MARY™ chip) has been developed at NOVA to meet the requirement of the digital mammography system [3]. Because the charge capacity requirement for good image quality exceeds the capabilities of standard CCD chips, this ASIC chip uses a slot-scanning, multi-section time delay integration (TDI) technique for dose efficient scatter rejection and the ability to use small detectors to produce a large area image. The MARY chip consists of 24 independent sections, each acting as a miniature CCD with eight rows for TDI. The signal from each section is combined off-chip to produce a full signal image. This chip is a good test platform where various x-ray detectors can be indium bump bonded on for testing. A p-channel process was used in the fabrication of the MARY chip and, therefore, it carries holes in its CCD wells, which is best suited for Si detectors.

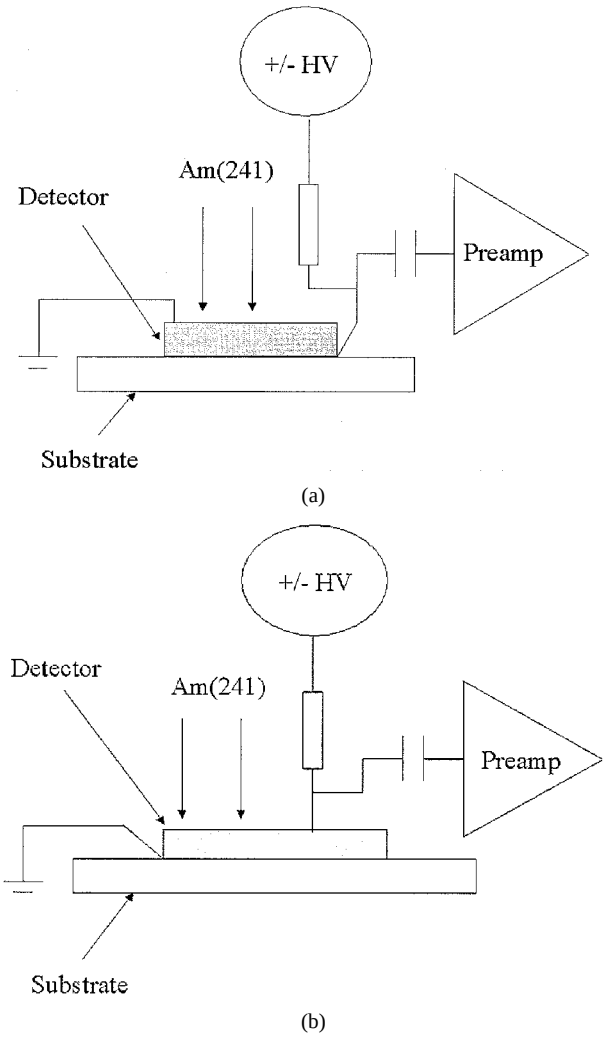

Fig. 1. Experimental setup for measuring spectroscopy responses from (a) backside irradiation and (b) frontside irradiation of a 0.5-mm-thick CdZnTe detector. The polarity of the shaper (not shown) is adjusted accordingly to accommodate the positive or negative pulses from the preamp.

Two CdZnTe detectors are tested. Both detectors are indium bump bonded onto the small version MARY chips, which have active areas of 192 $\times$ 128 pixels (9.6 mm $\times$ 6.4 mm). Each 192 pixel column is divided into 24 independent sections. Each section has eight TDI stages and a readout buffer. The small MARY chip produces an image of 128 lines. The 0.2 mm thick detector is from a polycrystal CdZnTe material and the 0.15 mm thick detector is from a single crystal CdZnTe material.

Two CdTe detectors are also tested. These detectors are fabricated using the same process as the CdZnTe detectors and have active areas of 192 $\times$ 384 pixels (9.6 mm $\times$ 19.2 mm), which fit the large version of the MARY chip. They produce images of 384 lines. They are polycrystalline material and are fabricated from the same batch CdTe material.

The MTF and DQE are measured in an x-ray system for mammography where the x-ray target is 40 cm away from the detector. A tantalum edge is translated across the detector during the x-ray exposure and the pre-sampled MTF is calculated using

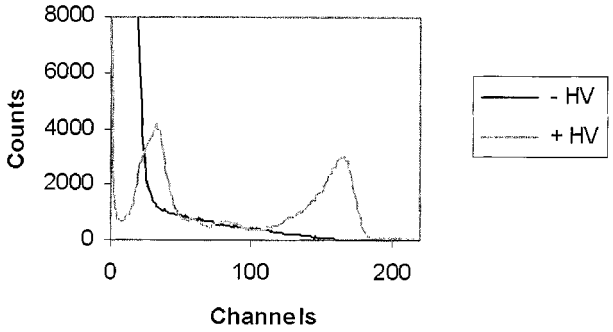

Fig. 2. Spectra comparison between hole-collecting mode (−HV) and electron-collecting mode (+HV) of a 0.5-mm-thick CdZnTe detector where the ^{241}Am source is placed at the backside. The total charge ratio of hole-collecting mode and electron-collection mode is 0.66.

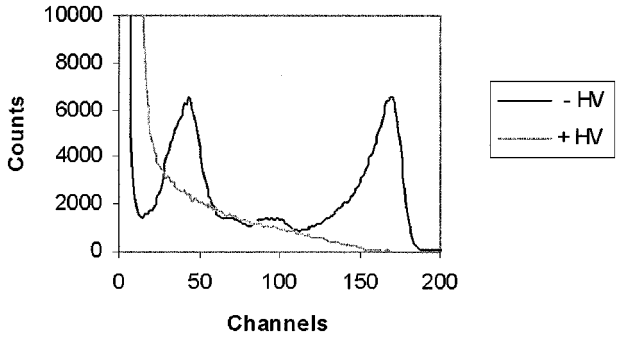

Fig. 3. Spectra comparison between hole-collecting mode (−HV) and electron-collecting mode (+HV) of the same CdZnTe detector where the ^{241}Am source is placed at the frontside. The total charge ratio of hole-collecting mode and electron-collection mode is 2.66.

an oversampled edge technique [2]. Noise properties are assessed using a simulated slit calculation on a flat-fielded image of a 6-mm-thick PMMA slab. From these data and the measured radiation exposure, the DQE of the imaging system is calculated [2].

For the polarization measurements, similar flat-fielded images are taken as described above, and the signal strengths are calculated after each x-ray exposure. The initial measurement is normalized to one for comparison with different detectors or test setups.

Samples are scanned under a computer-controlled step motor, with the scanning speed optimized for synchronization with the charge transfer speed inside the readout chip. Simple image processing techniques such as background subtraction, gain calibration, and contrast maximization are applied to images acquired in the test

III. Results

A. Detector Characterization

Fig. 2 is a typical ^{241}Am spectrum where the ^{241}Am source was placed at the backside of the detector [Fig. 1(a)]. We switched from electron collection mode to hole collecting mode by only reversing the high voltage and the polarity of the shaper. The gray curve represents the electron-collecting mode and the black curve represents the hole-collecting mode. We see a poor spectrum for hole collection because many holes were trapped traveling through the detector. We calculated the total charges collected in both cases under the same exposure time, and obtained a ratio of these two numbers which is 0.66. This suggests that about 1/3 of the charge was lost for hole-collecting configuration, if one assumes almost full-charge collection for the electron-collecting case.

We have also observed that a good spectrum can be obtained in a hole-collecting mode, as long as the irradiation is at the front side of the detector [Fig. 1(b)].

Fig. 3 shows spectra of the same setup, except that the ^{241}Am source is placed at the front side of the detector. A good spectrum was obtained for collecting holes. On the contrary, the electron-collecting mode yields poor spectrum. Again we calculated the total charge ratio of the two modes. For the electron-collecting mode holes had to travel through the detector to the back-side, and in this mode, we collected a total charge,

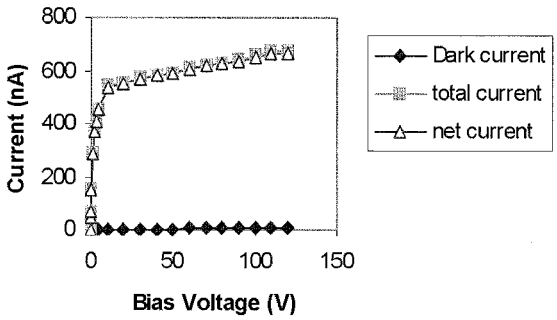

Fig. 4. X-ray current of a 0.5 mm poly crystal CdZnTe detector as a function of bias voltage. The x-ray was set at 30 kVp and 40 mA.

which is only about 38% of the good spectrum case, or the hole-collecting mode.

These results may be understood by keeping in mind that the photo-electric interaction is within a very shallow region underneath the electrode pad. If the holes move away to reach the other pad, they suffer severe loss due to trapping centers such as dislocations and defects. For the radioactive source ^{241}Am we used in the experiment, the major gamma peaks are a 59.5 keV energy peak with 36% relative strength and several 11–18 keV energy peaks with relative strength 39.5%. For CdZnTe, the linear attenuation coefficient for 60 keV and 15 keV gamma rays are 40 cm^{-1} and 270 cm^{-1}, respectively. The 60 keV gamma rays would be 64% absorbed within a 0.25 mm distance in CdZnTe and the same percentage of the 11–18 keV gamma rays would be absorbed within a distance of 0.04 mm. Therefore, the majority of electron–hole pairs are created within a 0.2 mm region from the irradiated surface of the detector. We believe that the short hole-propagation length in CdZnTe detectors causes the asymmetry in the spectroscopic responses between hole-collecting and electron-collecting modes.

For typical CdZnTe or CdTe materials, the mobility-lifetime products for holes are 10^{-5} cm^2/V and 10^{-4} cm^2/V respectively [5]. Therefore, for our hole-carrying readout chip, we should see better charge collection for the CdTe detectors.

Fig. 4 is a plot of the x-ray signal vs. bias voltage, for the 0.5-mm-thick CdZnTe detector. We see that there is a knee at a bias voltage of about 5 V, then the signal current increases slowly with increasing bias. The knee suggests the full collection of electrons, and the rising signal after that suggests that

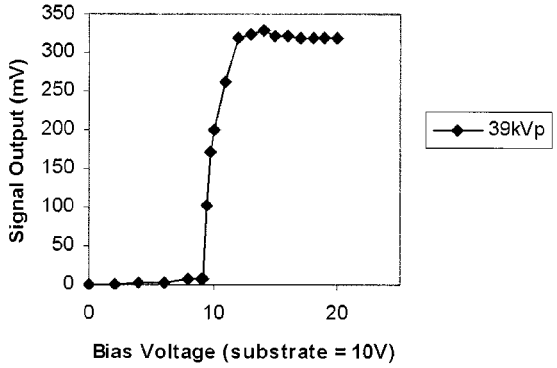

Fig. 5. X-ray signal versus bias voltage for a 0.15 mm CdTe detector hybridized to a MARY readout chip. The x-ray was set at 39 kVp and 32 mA.

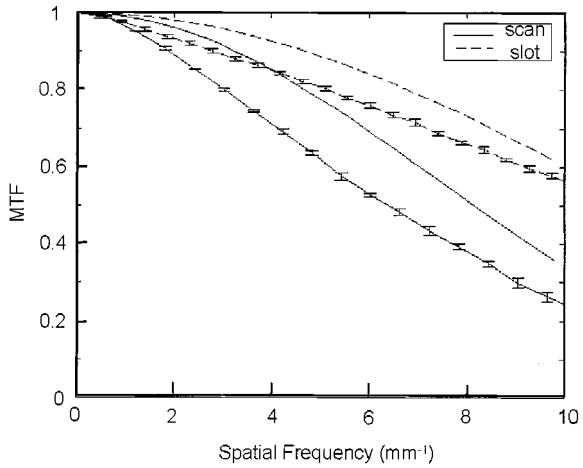

Fig. 6. MTF plots, both theoretical and experimental data, of a 0.2 mm polycrystal CdZnTe detector. The experimental data curves have error bars. The Nyquist limit of this detector is 10 lp/mm.

additional holes are still being pulled out from the traps making additional contribution to the signal.

Fig. 5 shows the x-ray signal measured on a 0.15 mm CdTe detector hybridized to a MARY readout chip. Since the substrate of the readout chip is at 9.6 V, the signal does not show up until the bias voltage is higher than that. With a relative bias about 3 V, we see a full signal output that is not increasing with additional bias. This suggests that charges are fully collected for this detector. We estimate that the hole propagation length at 3 V bias is about 0.2 mm, using mobility-lifetime product numbers given in reference [5], and the result agrees with our CdTe detector thickness, which is 0.15 mm.

B. MTF and DQE Measurements

The modulation transfer function (MTF) has been measured for a 0.2-mm-thick CdZnTe detector. Fig. 6 shows an MTF plot from the detector. The Nyquist frequency limit for this detector is 10 lp/mm, and we have obtained 25% in MTF at 10 lp/mm. Since we adopt a slot scanning technique, the MTF values in the scanning direction are always lower than those in the slot (non-scanning) direction, due to the temporal blurring of the moving scanning arm. In the MTF and DQE plots, we also include the theoretical simulation curves both in the slot and scan directions, which are based on earlier theoretical analysis [8], [9].

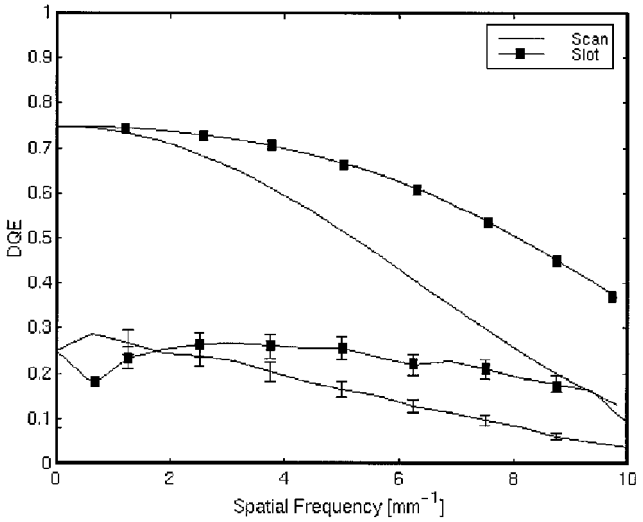

Fig. 7. DQE plots of a 0.2-mm-thick polycrystal line CdZnTe detector, for both theoretical prediction and experimental data. The measured DQE reaches only about 25% at zero spatial frequency. Dotted curves are in the slot direction and experimental data have error bars.

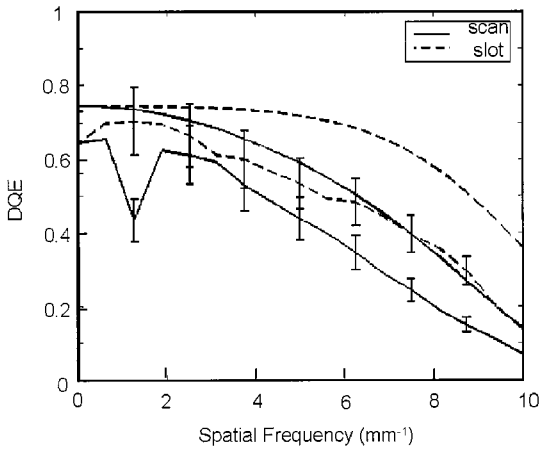

Fig. 8. DQE plots of a 0.15 mm thick single crystal CdZnTe detector. The DQE reaches about 65% at zero spatial frequency. The smooth curves without error bars are the theoretical simulations and the experimental data curves have error bars on them.

Because of the charge polarity of our present MARY readout chip (p-channel), holes were collected for the CdZnTe and CdTe detectors. This configuration caused losses for the charge signal in CdZnTe, as discussed earlier. Fig. 7 shows a DQE plot for a polycrystal CdZnTe detector, where the DQE gives only about 25% at zero spatial frequency. Improvement was obtained for a small single crystal CdZnTe detector, where the DQE reached 65% at zero spatial frequency, as is shown in Fig. 8.

In our earlier report [3], the DQE for silicon detectors varies from 55% to 75% at zero spatial frequency. We ascribe the poor DQE values for CdZnTe detectors to the incorrect charge collection mode, which results in about 30% to 60% charge collection loss. We are in progress to design our next version readout chip such that electrons are collected inside the readout chip (n-channel). Significant improvement in DQE is expected for the CdZnTe detector with the new readout chip.

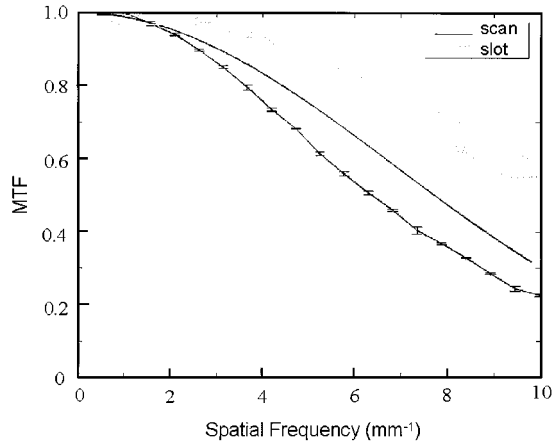

Fig. 9. MTF plot of a 0.15-mm-thick polycrystalline CdTe detector. The top two curves are theoretical and experimental data in the slot (nonscanning) direction and the lower two curves are the data in the scanning direction.

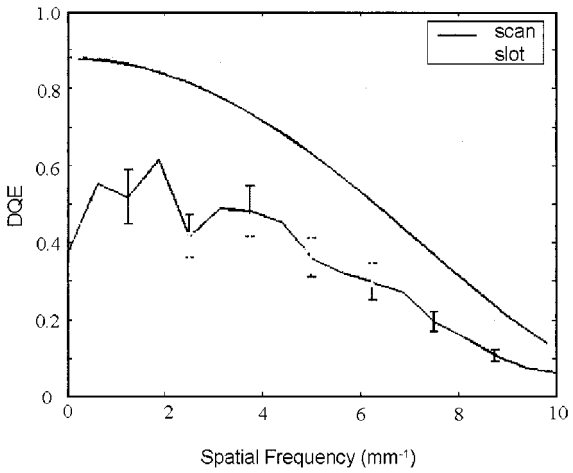

Fig. 10. DQE plot of a 0.15 mm polycrystalline CdTe detector at 26 kVp. The detector has shown polarization effect, which significantly increased the background noise. About 40% DQE is achieved at DC. The smooth curves are the theoretical simulations.

Fig. 8 shows the DQE plot of a 0.15 mm thick single crystal CdZnTe detector. Much improved DQE values were obtained, which is probably due to less trapping inside the detector.

Since CdTe has very similar detector properties compared to CdZnTe, we also fabricated 0.15 mm CdTe detectors and indium bump bonded them to our present hole-collecting MARY readout chips. The CdTe material was obtained from Eurorad (Strasbourg). Fig. 9 shows an MTF plot of a CdTe detector, which is similar to that of the CdZnTe detector.

C. Polarization of CdTe Detector

Since the hole-propagation length for CdTe is about ten times larger than that of CdZnTe, we expect to see further improved charge collection efficiency and thus DQE for this detector. Fig. 10 shows a DQE plot of a 0.15 mm CdTe detector, where the DQE at DC reaches only 40%. This low DQE value may be explained by some charge collection inefficiency, probably due to the polarization effect. CdTe detectors are known to have a polarization effect, where the accumulated charge inside the detector forms an internal field that reduces the external

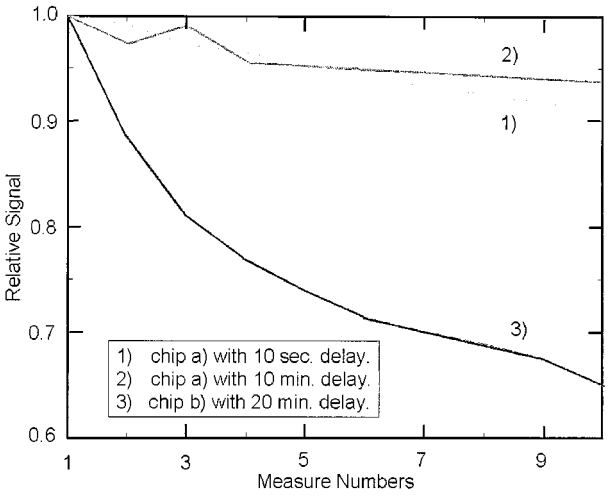

Fig. 11. Output signals versus number of x-ray exposures of two CdTe detectors. Curves 1) and 2) are from detector a) where 2) is at 10 minute x-ray exposure intervals and 1) is at 10 s time intervals. Curve 3) is from detector b) where the time interval is about 20 min.

bias field [6], [7]. Fig. 11 shows the detector output signal as a function of x-ray exposures. For detector (a), we see about 8% signal drop at x-ray exposures 10 s apart, but the signal drop is less at 5 min x-ray exposure intervals. For detector (b), we see clearly signal reduction, even though the waiting time between x-ray exposures is quite long. Results from Fig. 11 suggest that the present CdTe detectors have some polarization effect, which decreases the charge collection efficiency and, thus, causes low DQE measurements. We can also see that this polarization effect has sample dependence. The two samples shown in Fig. 11 were made from the same batch of CdTe materials using the same fabrication process, yet their polarization behaviors are different: Sample (b) shows a stronger reduction of the signal strength. How to control the yield of low polarization detectors remains a challenging task for future application of this material.

Several improvements could be done to reduce the polarization effect in CdTe. For the present CdTe material we used, the resistivity is less than 10^9 ohm-cm, and the dark current limits the maximum bias voltage to only several volts. If we can improve the resistivity of the CdTe material, then higher bias field can effectively reduce the polarization. A properly designed metal contact can also reduce the polarization effect [6].

D. Image Studies

Fig. 12 shows image comparisons of a mosquito fish image taken from a 0.15-mm-thick CdZnTe detector and a 0.15-mm-thick CdTe detector. The top image is from the CdZnTe detector and the bottom one is from the CdTe detector. The fish is about 20 mm in length and we see clear bone structure of the fish in both pictures. The CdTe image seems to have a slightly poorer image quality than the CdZnTe one, which might be due to the polarization effect in the CdTe material that causes higher back ground noise.

The present slot-scanning detector system can easily be applied to other medical imaging applications such as digital radiography, if the detector thickness is properly selected to stop the

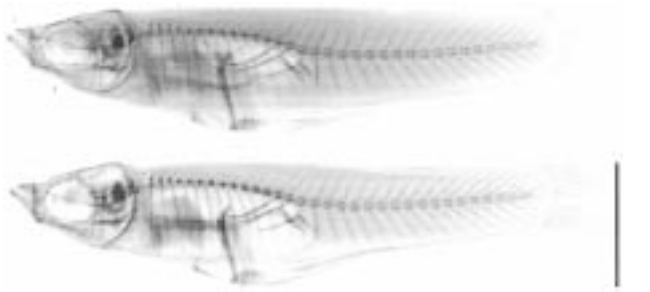

Fig. 12. Images of a mosquito fish from a 0.15-mm-thick CdZnTe detector (top) and a 0.15-mm-thick CdTe detector (bottom). The x-ray was set at 30 kVp and 40 mA. The length of the fish is about 20 mm.

particular energy range x-ray photons. For industrial imaging applications such as NDE and NDI, the silicon detector systems can be applied to less critical scanning applications because of the low cost of the detectors. The CdZnTe or CdTe detectors can be applied to critical imaging applications where both high resolution and high efficiency are required.

IV. Discussion and Summary

In Fig. 3, the detector configuration is changed and thus the input noise is different from that in Fig. 2. The exposure time is also different and therefore it is difficult to compare the results to those in Fig. 2. The relative total charge collections are significant for each figure because they are taken under the same system configuration and have the same exposure time.

Our test results show that CdZnTe and CdTe are good materials for radiation detection. Excellent results are obtained for both materials. Due to the readout chip limitation, holes are collected for these detectors. The CdTe detectors have longer hole-propagation lengths which should improve charge collection efficiency for hole collection. However, polarization effect reduces its performance. Improved detector resistivity or contact metallization may reduce this effect. To utilize the maximum potential of the CdZnTe detector, an electron version of the readout chip is necessary for good charge collection efficiency, which will result in even better DQE than those presented here.

We have demonstrated that the DQE values of the CdTe and CdZnTe detectors could reach 40% and 60% above, respectively. These detectors have potentials for even higher DQE values with improved fabrication techniques or readout devices. These values are superior than those from screen-films or scintillator based digital systems, which are typically around 30–40% [2]. A major task for our future work is to redesign the readout chip such that electrons will be transported. A multidetector arm is also under construction where full breast size images could be obtained. We believe that a highly efficient high-resolution digital mammography system will help to reduce the false positive and false negative readings of the current mammograms, and, therefore, help female patients in their early detection of breast cancer.

References

[1] S. A. Feig and M. J. Yaffe, "Digital mammography, computer-aided diagnosis, and telemamography," *Radiolog. Clinics North America*, vol. 33, pp. 1205–1230, 1995.

[2] N. L. Ford, J. G. Mainprize, S. Yin, T. O. Tümer, E. E. Gordon, W. J. Hamilton, and M. J. Yaffe, "Comparison of different detector materials for digital mammography," in *Proc. 5th Int. Workshop Digital Mammography*, Toronto, ON, Canada, June 2000, p. 39.

[3] S. Yin, T. O. Tümer, D. Maeding, J. Mainprize, G. Mawdsley, M. J. Yaffe, and W. J. Hamilton, "Hybrid direct conversion detectors for digital mammography," *IEEE Trans. Nucl. Sci.*, vol. 46, pp. 2093–2097, Dec. 1999.

[4] M. J. Yaffe and J. A. Rowlands, "X-ray detectors for digital radiography," *Phys. Med. Biol.*, vol. 42, pp. 1–39, 1997.

[5] C. Szeles, E. E. Eissler, D. J. Reese, and S. E. Cameron, "Radiation detector performance of CdTe single crystal grown by the conventional vertical Bridgman technique," *Proc. SPIE*, vol. 3768, p. 98, 1999.

[6] R. O. Bell, G. Entini, and H. B. Serreze, "Time-dependent polarization of CdTe gamma-ray detectors," *Nucl. Instrum. Meth.*, vol. 117, pp. 267–271, 1974.

[7] H. L. Malm and M. Martini, "Polarization phenomena in CdTe: Preliminary results," *Can. J. Phys.*, vol. 51, p. 2336, 1973.

[8] J. G. Mainprize, M. J. Yaffe, T. O. Tümer, S. Yin, and W. J. Hamilton, "Design considerations for a CdZnTe digital mammography system," in *Proc. 4th Int. Workshop Digital Mammography*, Nijmegen, The Netherlands, 1998, pp. 19–26.

[9] J. G. Mainprize, N. L. Ford, Nancy, S. Yin, T. O. Tümer, and M. J. Yaffe, "Image quality of a prototype direct conversion detector for digital mammography," *Proc. SPIE*, vol. 3659, pp. 398–406, 1999.